Application of Spectral Decomposition Methods to the Definition of Stratigraphic Features Associated with Channel Reservoirs in the Southeast Petroleum Province, México

Article *in* Pure and Applied Geophysics · September 2018

DOI: 10.1007/s00024-018-1999-2

Vsevolod Yutsis
Instituto Potosino de Investigación Científica y Tecnológica

Pure Appl. Geophys.

https://doi.org/10.1007/s00024-018-1999-2

Pure and Applied Geophysics

Application of Spectral Decomposition Methods to the Definition of Stratigraphic Features Associated with Channel Reservoirs in the Southeast Petroleum Province, México

Fernando Alvarez San Román[1] and Vsevolod Yutsis[2]

Abstract—Spectral decomposition transforms seismic data into the frequency domain via mathematical methods such as the discrete Fourier transform, S-transform, time–frequency continuous wavelet transform and continuous wavelet transform. The transformed results include tuning cubes and a variety of discrete common frequency cubes, which reveal structural and stratigraphic features, such as channels, thin bed reflections, and subtle faults. When a spectral decomposition algorithm is applied to seismic reflection data, it breaks down the seismic signal into its frequency components and this allows visualization of the data at specific frequencies, and identification of stratigraphic and structural features that would otherwise be overlooked in full bandwidth displays. The stratigraphic features delineated through the different algorithms, such as channels and their sedimentary facies, could be related to the presence of reservoir rock, i.e., underground rock units where the oil migrates and accumulates. An example from the Southeast Petroleum Province in México is presented.

Key words: Spectral decomposition, channels, discrete Fourier transform, S-transform, time–frequency continuous wavelet transform, continuous wavelet transform.

1. Introduction

Where conventional seismic processing generally has a resolution of 20 m or more, spectral decomposition can provide a resolution of 10 m or less. Therefore, spectral decomposition is a particularly helpful technique for analysing thinly bedded reservoirs and delineating depositional features such as channels. Spectral decomposition unravels the seismic signal into its constituent frequencies. This allows the interpreter to see amplitude and phase tuned to specific wavelengths, just as a radio can pick out a single station. Since the stratigraphy resonates at wavelengths dependent on the bedding thickness, the interpreter can not only image subtle thickness variations and discontinuities, but also accurately predict bedding thickness quantitatively (Partyka et al. 1999). In addition, since the high-frequency response of a reflector can be attenuated by the presence of compressible fluids, spectral decomposition can also assist in the direct detection of hydrocarbons (Castagna et al. 2003). These approaches, applied alone to a seismic dataset, can be very enlightening, but the results can also be somewhat cryptic. Seismic modelling gives the interpreter critical insight into tuned attribute maps, and allows predictions of what a particular bed geometry or thickness trend will look like. Volume visualization and interpretation can enhance the interpretation further, significantly reducing exploration risk. This paper shows how the application of spectral decomposition methods like the discrete Fourier transform (DFT), the continuous wavelet transform (CWT), the time–frequency continuous wavelet transform (TFCWT) and the S-transform (ST) applied to seismic data from the Southeast Petroleum Province give to the explorationist the ability to quickly and easily perform structural and stratigraphic interpretations in complex geological conditions associated with the presence of salt and faults that can even affect the seismic reflectivity. Thus, the application of these four different methods is of great relevance because this is the most prolific oil and gas province in Mexico.

[1] Universidad Autónoma de Nuevo León, Facultad de Ciencias de la Tierra, Carretera a Cerro Prieto km 8, Ex-Hacienda de Guadalupe, 67000 Linares, Nuevo León, Mexico. E-mail: fernando1511@hotmail.com

[2] División de Geociencias Aplicadas, Instituto Potosino de Investigación Científica y Tecnológica, Camino a la presa San José No. 2055, 78216 San Luis Potosí, SLP, Mexico. E-mail: vsevolod.yutsis@ipicyt.edu.mx

Published online: 25 September 2018

Birkhäuser

2. Geological and Structural Settings of the Southeast Petroleum Province

The Southeast Petroleum Province is subdivided into three geological provinces, each one with its own characteristics (Fig. 1).

2.1. Salina del Istmo

Salina del Istmo (Fig. 2a) corresponds to the southern portion of the Salina del Istmo Province. It extends from the front of the Sierra de Chiapas in the south to the 500-m bathymetric contour in the north, abutting the Veracruz Basin to the west and the Pilar Reforma-Akal to the east. This province includes, in its southeast portion, the Comalcalco Sub-basin, due to its association with sediment loading and salt evacuation. Structurally, it is characterized by diapirs, walls, tongues and awnings of salt that gave rise to the formation of basins by evacuation of salt, such as the one at Comalcalco, and mini-basins between salt bodies. Mesozoic and Paleogenic rocks have been

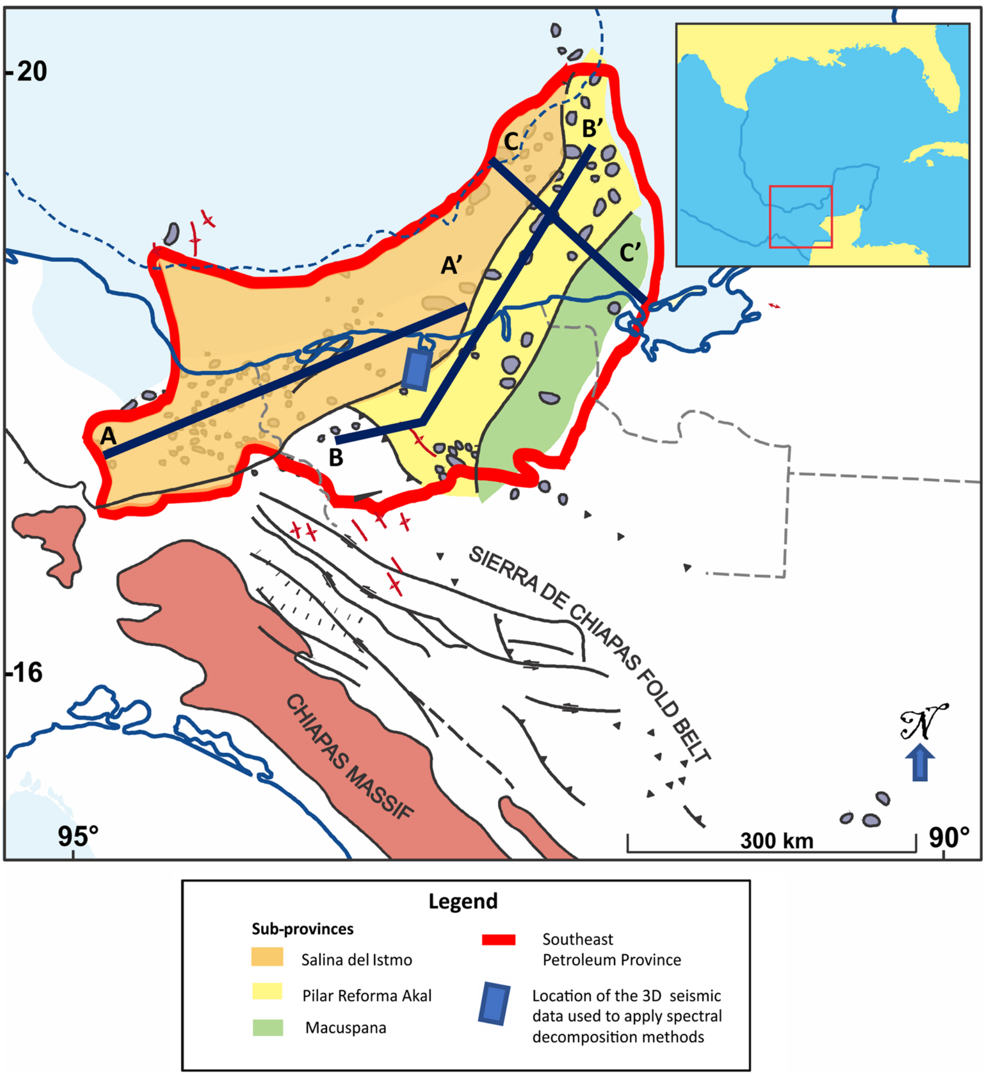

Figure 1
Location of the Southeast Petroleum Province and location for the area of the 3D seismic data used to calculate maps with the different spectral decomposition methods

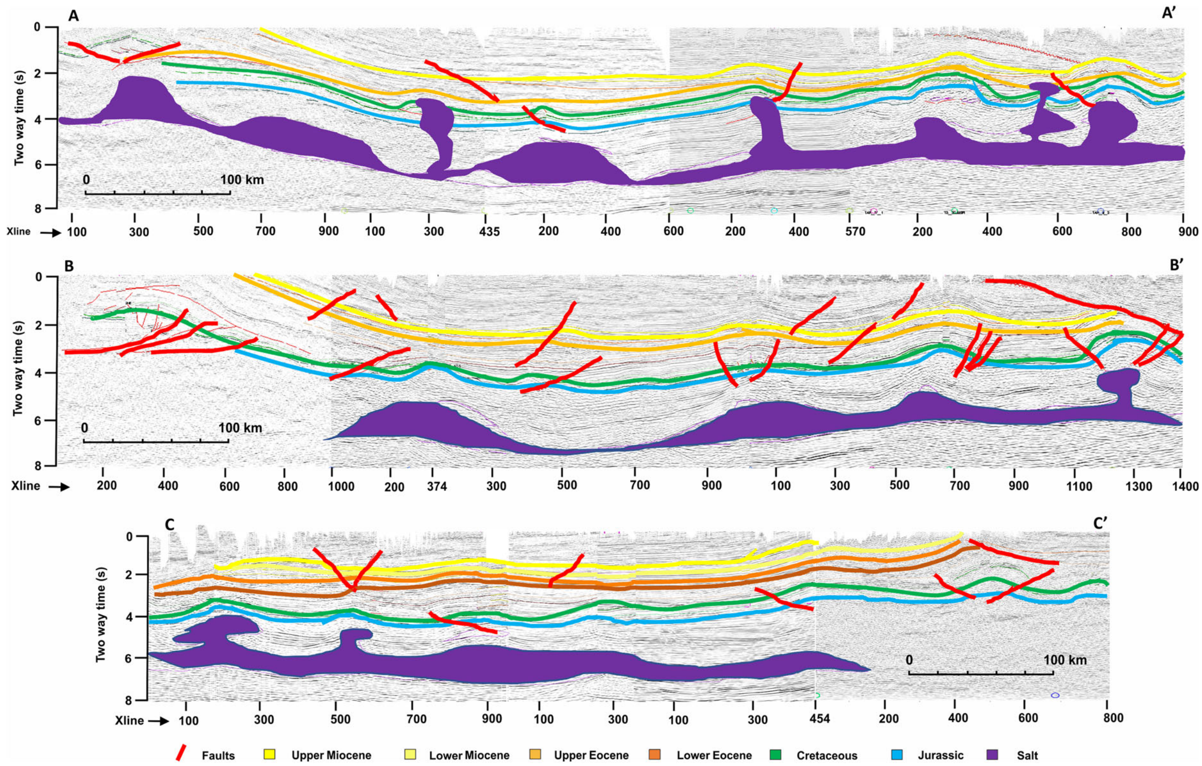

Figure 2
a Structural section A–A′ of the Salina del Istmo Province (see Fig. 1 for location). **b** Structural section B–B′ of the Pilar Reforma-Akal Province (see Fig. 1 for location). **c** Structural section C–C′ of the Macuspana Province (see Fig. 1 for location)

deformed either by folding and faulting with a northeast-southwest strike and vergence toward the northwest, or by rotation on the pedestals of saline diapirs. Tertiary structures are associated with saline masses, with north-west striking faults that affect even the Mesozoic and listric faults with a dip to the southeast (Oviedo-Pérez 1998; Robles-Nolasco et al. 2004; Soto-Cuervo et al. 2004).

2.2. *Pilar Reforma-Akal*

Pilar Reforma-Akal (Fig. 2b) is bordered to the west by the Comalcalco fault system and to the east by the Frontera fault system, the lineament of Amate-Barrancas clay diapirs and the Topén–Níspero fault. To the south, it bounds the fold belt of the Sierra de Chiapas, and to the north, the Yucatán Platform. Within this province, there are overlapping structural styles. The first is characterized by rotated and faulted blocks and salt rollers of Late Jurassic-Early Cretaceous age, located on the eastern marine edge of the Pilar Reforma-Akal. The second is related to compression of the sedimentary cover of middle-late Miocene age. The third and most important is represented by folds and thrusts striking northwest-southeast with vergence to the northeast and of mid-late Miocene age, which take off in clayey and evaporitic horizons of the Oxfordian and Callovian, affecting Mesozoic, Paleogene and Early Miocene strata. The latter, identified within the Neogene, corresponds to a style of faults with a north-west dip, which take off at the Oligocene-Miocene boundary (Ángeles-Aquino et al. 1994; González et al. 2004; Martínez-Kemp et al. 2005).

2.3. *Macuspana*

Macuspana (Fig. 2c) is bounded to the east-southeast by a system of normal faults that separates it from the Yucatan Platform, with the Xicalango

Fault. To the northwest-west, it borders the Frontera Fault system, the Amate-Barrancas diaphyric alignment and the Topén–Níspero Fault. To the south, it abuts the Chiapas fold belt. This sub-province is characterized by early Miocene-Pliocene faults striking northeast-southwest that dip to the northwest with rollover anticlines associated with the evacuation of Oligocene clays. In the marine portion, these faults displace Mesozoic rocks to the northwest as a system of "rafts" in contact with Jurassic salt and Oligocene sediments.

3. Spectral Decomposition Methods

Spectral decomposition refers to the transformation of seismic data into individual frequency components within a seismic bandwidth (Guo et al. 2009). Using multiple spectral decomposition techniques can help to visualize different aspects of reservoir morphology, and can greatly improve understanding of reservoir potential; the choice of the best method depends on the geological problem that is being addressed. The resolution capabilities of each method vary. Therefore, it is necessary to know what resolution is required to delineate a reservoir in its geological setting.

This section outlines the differences between four methods, and the advantages and disadvantages of each technique, using a seismic horizon that was obtained by manually picking an easily recognizable peak along each of ten lines in the north–south and east–west direction and then interpolating the picks (Marfurt and Kirlin 2001). Spectral decomposition maps from a channel reservoir in the Southeast Petroleum Province are used to illustrate the four methods.

3.1. Discrete Fourier Transform

Conventional spectral decomposition is performed using the DFT, which is preferred for evaluating the spectral characteristics of a long window containing many events (Castagna and Sun 2006). The DFT is a widely used spectral decomposition algorithm that uses a fixed window approach. In this method, the user specifies the length of a time window in which the signal is transformed to represent the acoustic properties and bed thicknesses within the window. Longer window lengths sample a wider range of data and might produce a better statistical representation of the acoustic properties. The downside is that fine-scale events are not resolved if the window length is too long. By sampling the seismic signal with a short window size, the averaging effects inherent in the fixed-window method can be avoided and better frequency resolution can be obtained. The shorter window lengths can help resolve high-frequency events and separate events with similar or closely spaced dominant frequencies. However, these shorter windows can overlook events at lower frequencies and compromise map resolution. Figure 3 shows the map, section and frequency gather results of the DFT at 24 Hz. In map view, the DFT results resolve the channel better than the poststack data, but only give a partial picture of the channel morphology.

3.2. Continuous Wavelet Transform

The CWT samples the seismic signal using a moving, scalable time window where the wavelets dilate in such a way that the time supports changes for different frequencies (Sinha et al. 2005). In this method, the window size automatically changes with frequency, and allows adaptive sampling of the seismic trace. The resulting spectral maps provide higher temporal resolution at higher frequencies compared to the DFT.

The example in Fig. 4 shows map, section and frequency gather results of a CWT spectral decomposition at 24 Hz. The CWT frequency gather shows that the CWT is far superior in preserving reflection events than the DFT method for higher frequencies. At lower frequencies, however, the CWT cannot adequately resolve events that are closely spaced in the time domain.

In map view, the CWT results resolve the channel better than in the poststack data and reveal the channel morphology significantly better than the DFT map in the previous section. These results are consistent with the frequency gather analysis, which demonstrates that the moving window calculation of the CWT provides higher resolution than the DFT.

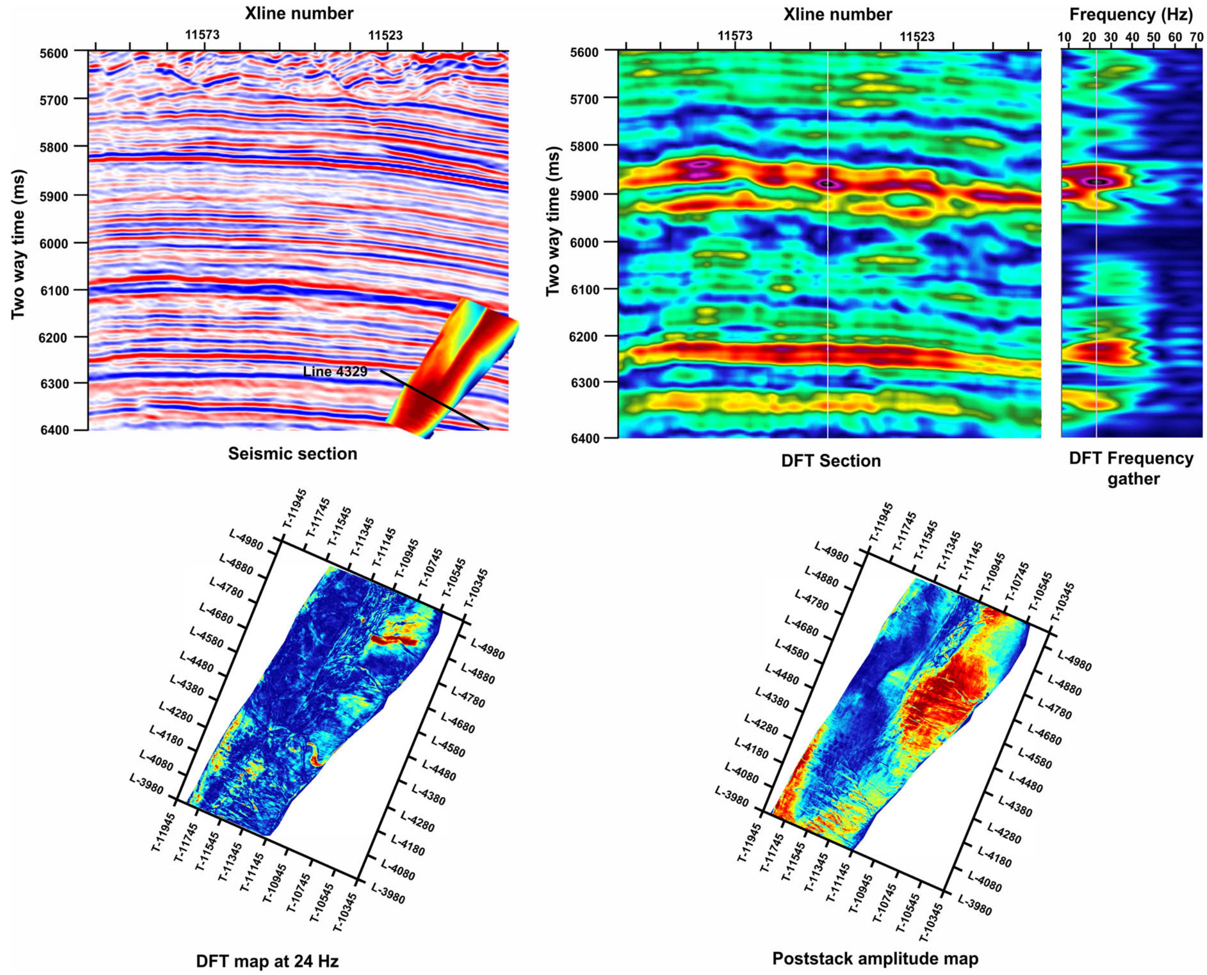

Figure 3
Example: spectral decomposition using the DFT. This figure shows the original seismic section on which the spectral decomposition method was applied. The DFT section and the frequency gather show the amplitude values in ranks from 10 to 70 Hz, which can be compared with the DFT map at 24 Hz and the poststack amplitude map

3.3. Time–Frequency Continuous Wavelet Transform

A time–frequency CWT (TFCWT) generates a time–frequency map that displays the exact frequency for any event and can be used to interpret seismic data in the frequency domain (Sinha et al. 2005). The CWT and DFT methods, on the other hand, output maps at a central frequency within a given time window. For example, a CWT spectral decomposition map at 24 Hz displays the average amplitude response from around 20–30 Hz. However, a TFCWT map at 24 Hz shows the amplitudes at exactly 24 Hz. Like the CWT, the TFCWT spectral decomposition method uses a moving window approach, but it does not average neighbouring frequencies in the same way as the previously mentioned methods. Therefore, TFCWT maps provide higher time–frequency resolution than those for the DFT or CWT. Both the CWT and TFCWT methods provide high-frequency resolution at low frequencies, and high temporal resolution at high frequencies.

One disadvantage of a TFCWT is that it is computationally intensive, so generating spectral decomposition maps with this method can be time-consuming. The example in Fig. 5 shows map,

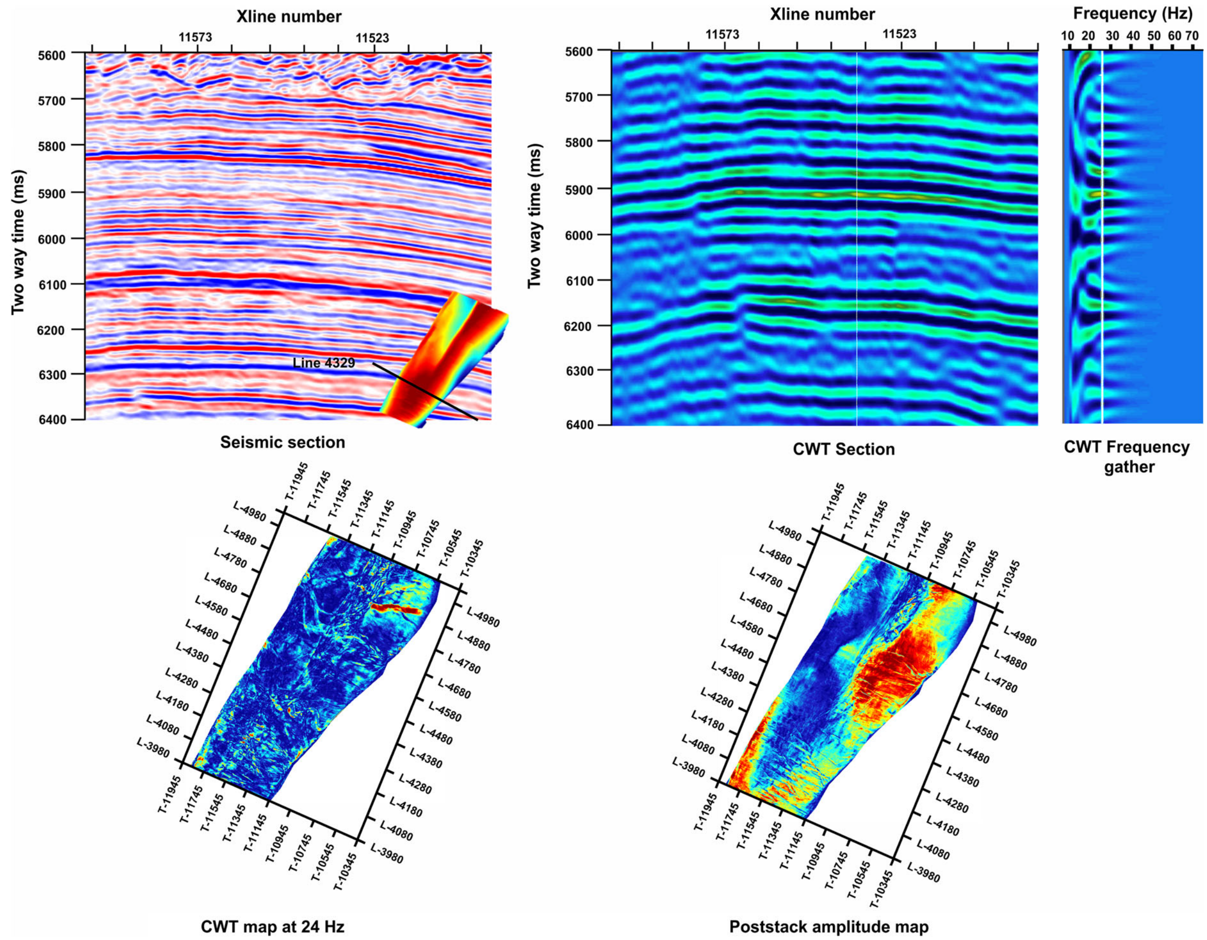

Figure 4

Example: spectral decomposition using the CWT. This figure shows the original seismic section on which the spectral decomposition method was applied. The CWT section and the frequency gather show the amplitude values in ranks from 10 to 70 Hz, which can be compared with the CWT map at 24 Hz and the poststack amplitude map

section and frequency gather results of TFCWT spectral decomposition at 24 Hz. Because of the instantaneous spectrum calculation of the TFCWT, better resolution and greater detail within the channel complex can be seen. In map view (Fig. 5), the TFCWT results resolve the channel much better than the poststack data, and reveal the channel morphology significantly better than either the DFT or CWT maps.

3.4. *S-Transform*

Like the TFCWT, the ST generates a real time–frequency map and samples the seismic signal with a moving time window. However, the size of the window in the ST method is frequency-dependent. Because the transform has a more rigorous relationship with the spectra, it can produce spectral decomposition maps with fairly high resolution. An ST is faster to calculate than a TFCWT but can produce similar results and the ST has high stability in noisy conditions (Stockwell et al. 1996).

The example in Fig. 6, shows map view and frequency gather results of an ST spectral decomposition at 24 Hz. In this case, the ST frequency gather and map are almost identical to the TFCWT results (see Sect. 3.3). However, this might not always be the case.

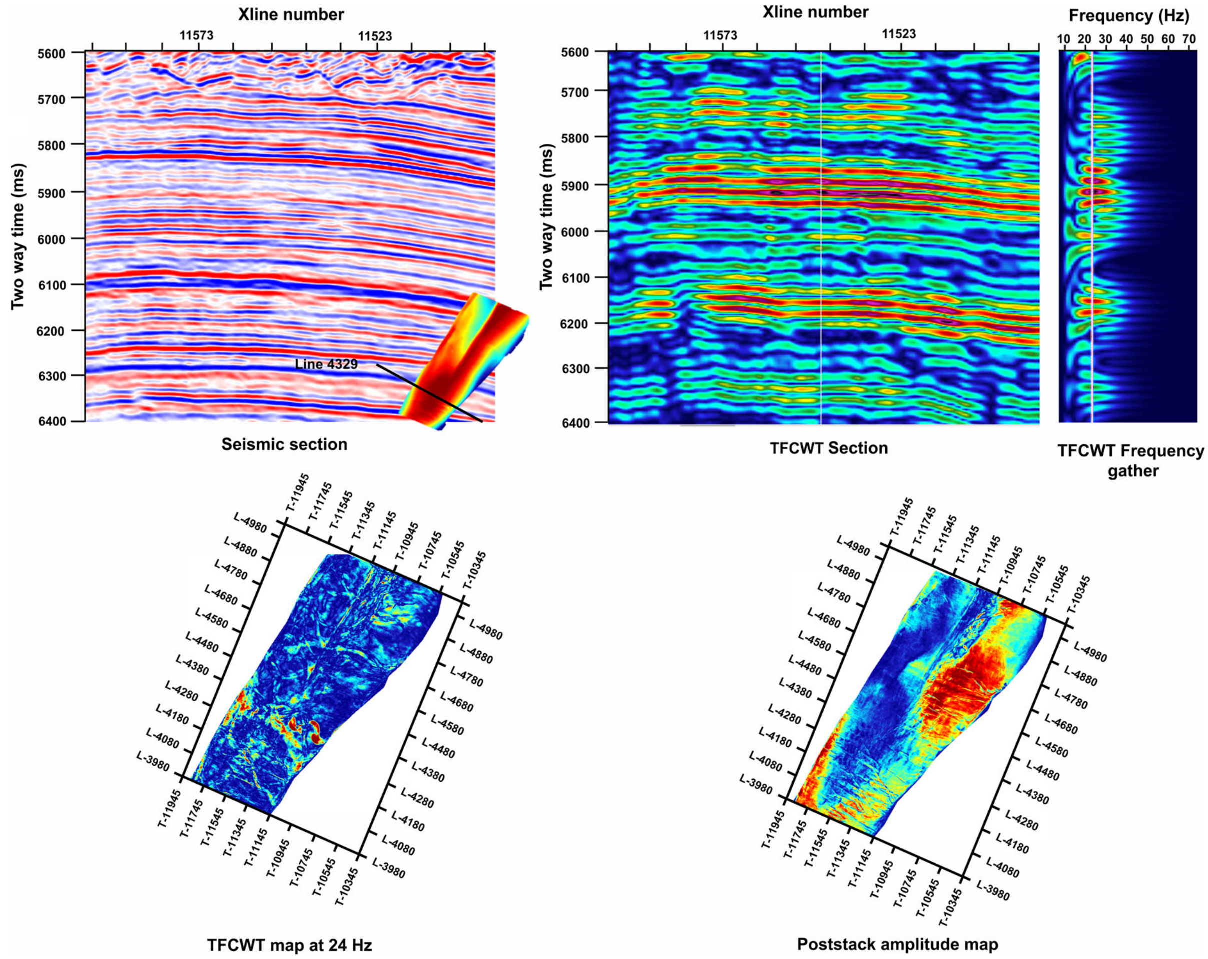

Figure 5
Example: spectral decomposition using the TFCWT. This figure shows the original seismic section on which the spectral decomposition method was applied. The TFCWT section and the frequency gather show the amplitude values in ranks from 10 to 70 Hz, which can be compared with the TFCWT map at 24 Hz and the poststack amplitude map

4. *Comparing Spectral Decomposition Methods*

A summary of spectral decomposition methods including windowing approach, advantages and disadvantages is shown at the Table 1.

4.1. Frequency Gathers

Comparing the frequency gathers generated from each method demonstrates the differences in frequency resolution among the four techniques. The purpose of the vertical seismic section analysis of the spectral decomposition is to compare the response of sands with various frequency ranges (Naseer 2014). Figure 7 shows four frequency gathers from different spectral decomposition transforms. Each gather was generated from the same trace location. Moving from left to right, the increasing resolution of the signal in the frequency domain can be seen. The DFT gather shows that the events are smudged or blurred because of the effect of averaging the signal response over a fixed window.

The CWT gather provides increased resolution and separates individual events better than the DFT gather. This is possible because the moving window of the CWT transform enables adaptive sampling of the trace, and a better representation of the signal within the window. The TFCWT and ST give the best

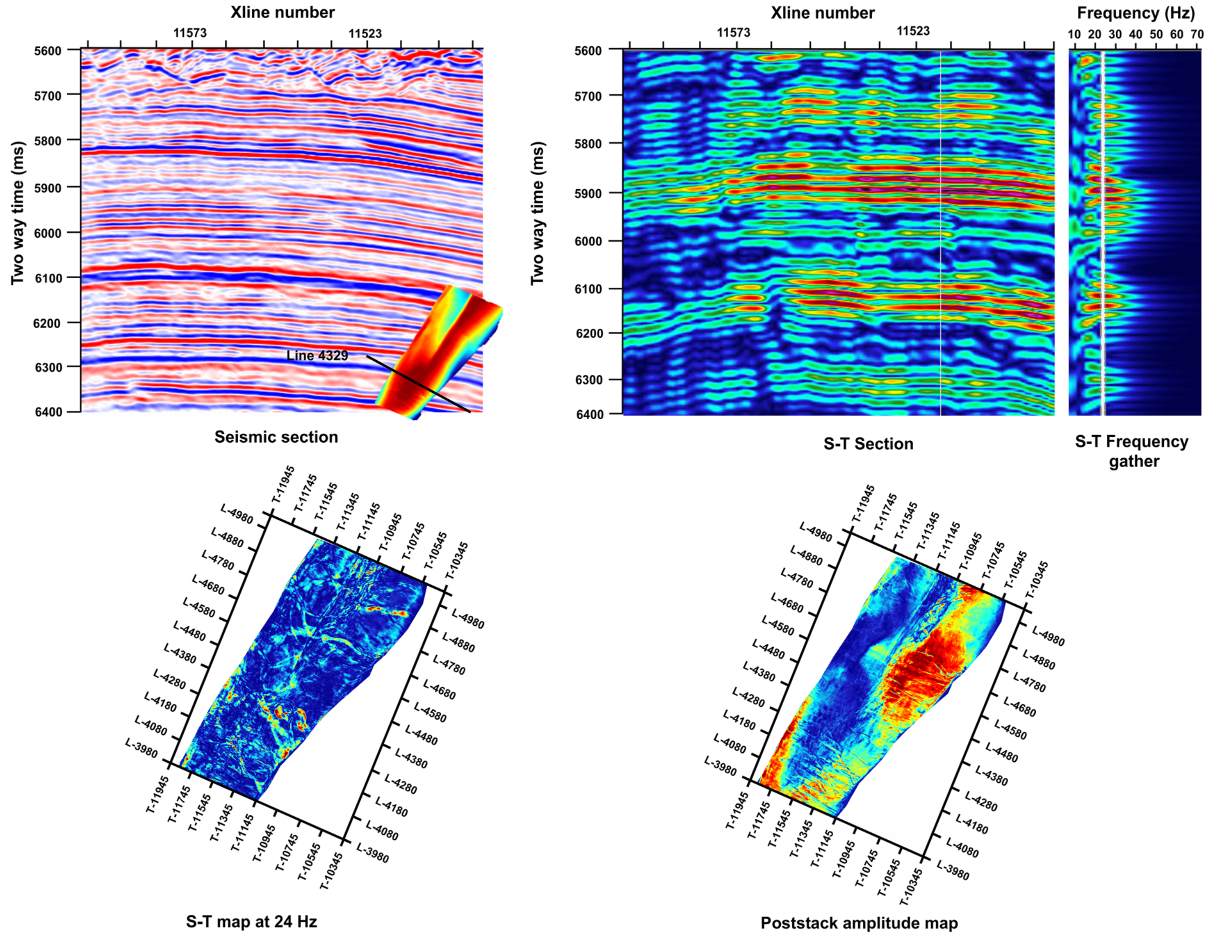

Figure 6
Example—spectral decomposition using S-transform. This figure shows the original seismic section on which the spectral decomposition method was applied. The ST section and the frequency gather show the amplitude values in ranks from 10 to 70 Hz, which can be compared with the ST map at 24 Hz and the poststack amplitude map

resolution and detail for spectral decomposition data analysis. This is because both the TFCWT and ST generate time–frequency maps that display the exact frequency for any event. Alternatively, the CWT and DFT methods produce maps at a central frequency within a given time window.

4.2. *Spectral Maps*

Using the Southeast Petroleum Province channel reservoir as an example, and using principles of geomorphology, calibration of the patterns through conventional interpretation of the seismic section and the use of colours in order to delineate the channels (Liu and Marfurt 2007), the four spectral decomposition methods are observed to provide better resolution of the channel morphology compared to the poststack amplitude map (Fig. 8a). However, each method provides a different spectral response at 24 Hz. Figure 8b shows spectral decomposition results via a DFT with a window size of 30 ms. The map shows some detail in the channel morphology, but does not resolve the entire channel at 24 Hz. Figure 8c, d demonstrates that the moving window approaches of the CWT and TFCWT provide improved time–frequency resolution compared to the DFT. However, the TFCWT map has a better differentiation of relative thicknesses within the

Table 1

Summary of spectral decomposition methods

Spectral decomposition method	Windowing approach	Advantages and disadvantages
Discrete Fourier transform (DFT)	Fixed-time window	Short windows can resolve high frequency events, but might overlook low-frequency events Longer windows average the response to get better statistical representation, but might overlook fine details
Continuous wavelet transform (CWT)	Moving, scalable time window Window size automatically changes with frequency	Allows adaptive sampling of a trace, which preserves some events better than DFT Cannot adequately resolve low frequency events that are closely spaced in time domain
Time–frequency CWT (TFCWT)	Moving, scalable time window (like CWT) window does not average neighbouring frequencies	Generates a real time–frequency map, with higher resolution than CWT for a time–frequency spectrum
S-transform (ST)	Moving, *f*-dependent time window Window length is decided by the frequency (has more rigorous relationship with *f* than CWT or TFCWT)	Results are similar to TFCWT, with higher resolution than CWT for a time–frequency spectrum

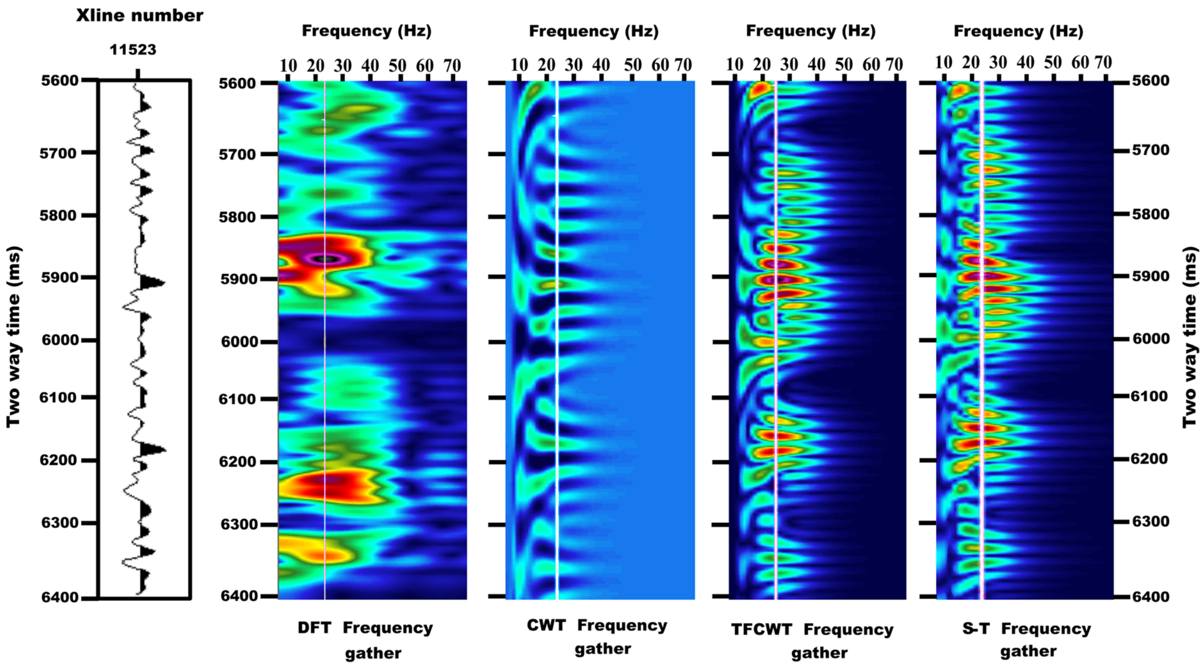

Figure 7
Seismic trace 11,523 extracted from the original seismic section used in each method and a comparison between the DFT, CWT, ST and TFCWT frequency gathers

channel. The ST map produced similar results to the TFCWT, with only slightly less resolution (Fig. 8e). Overall, the TFCWT map resolves the channel morphology with greater detail compared to the other methods used here. A review of the four spectral decomposition maps shows that the results are consistent with the frequency gather analysis.

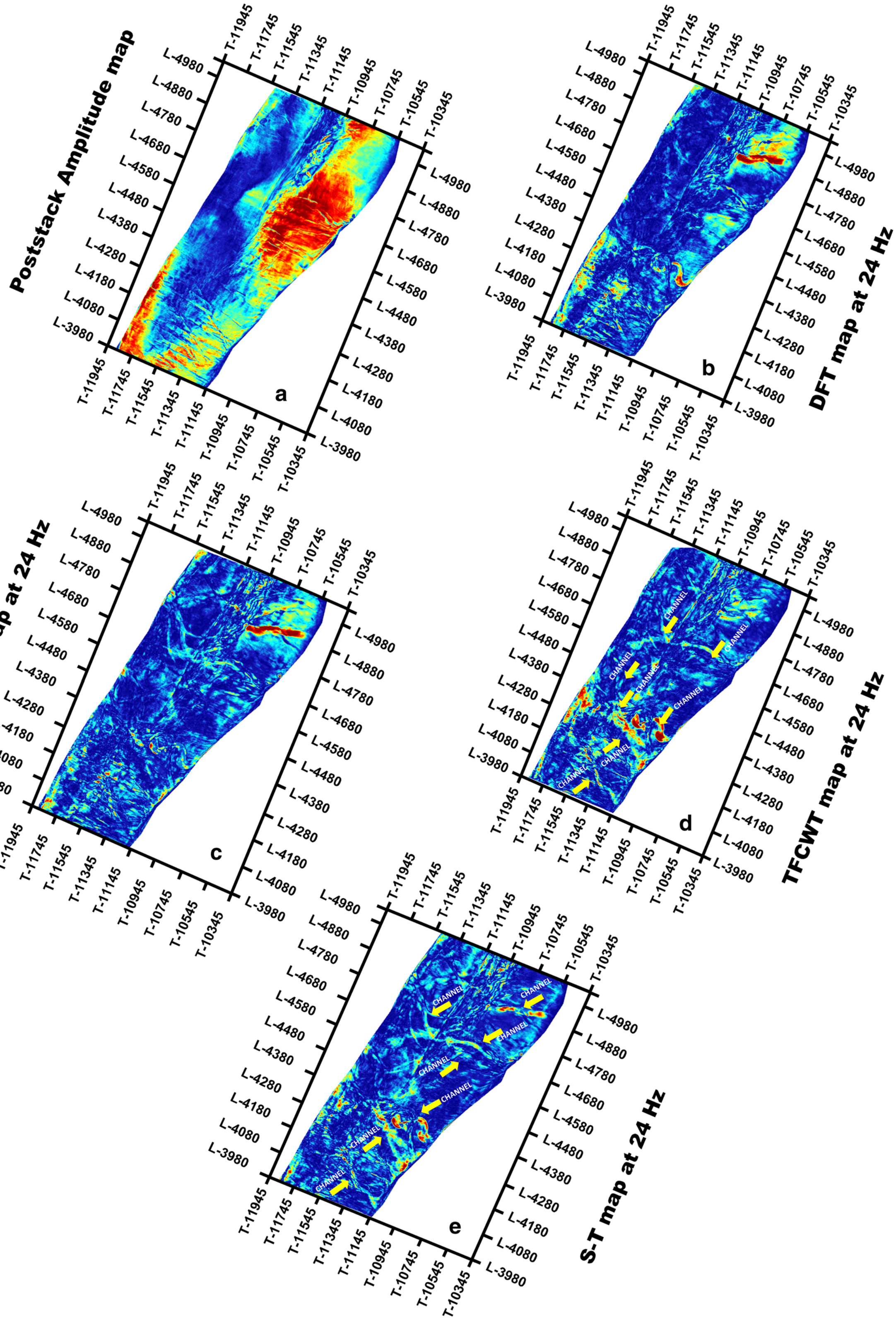
Poststack Amplitude map
a
DFT map at 24 Hz
b
CWT map at 24 Hz
c
TFCWT map at 24 Hz
d
S-T map at 24 Hz
e
CHANNEL
L-4980
L-4880
L-4780
L-4680
L-4580
L-4480
L-4380
L-4280
L-4180
L-4080
L-3980
T-11945
T-11745
T-11545
T-11345
T-11145
T-10945
T-10745
T-10545
T-10345

◀Figure 8
Spectral maps comparing spectral decomposition. This figure shows the different responses for the four spectral decomposition methods based on the original in **a**. Yellow arrows in **d** and **e** indicate the channel morphology

5. Conclusions

In imaging the Southeast Petroleum Province channel sands, running multiple spectral decomposition methods helped to resolve the channel morphology and bed thickness relationships within the channel facies. Although the TFCWT spectral decomposition provided the best resolution, it also took the longest time to calculate. The ST maps provided similar results to the TFCWT that were generated more quickly, making the ST method the most efficient technique for resolving the channels in this study.

Spectral decomposition can greatly improve visualization and interpretation workflows by revealing thin beds, lateral discontinuities, and subtle anomalies not readily identified in poststack data. By correlating the spectral maps back to well logs and attribute relationships, the technique can help the interpreter achieve a better understanding of complex reservoir plays, and thus plan drilling strategies with greater confidence.

Acknowledgements

The 3D seismic data used here came from Petroleos Mexicanos (Pemex Exploration), who collected and paid for the seismic data and gave authorization for the use of this information through the document PEP-SE-AT-704-2013. The authors are also grateful to the sponsors of the Pemex CTA (Administrative Technical Center) for permission to use their institutional interpretation software, Decision Space Desktop. The authors are grateful to Dr. Aaron James Martin for his helpful comments and remarks and a special thanks to the two anonymous reviewers for their valuable comments and suggestions which helped to improve the manuscript.

References

Ángeles-Aquino, F. J., Reyes-Núñez, J., Quezada-Muñetón, J.M., & Meneses-Rocha, J. J. (1994). *Tectonic evolution, structural styles, and oil habitat in Campeche Sound* (Vol. 44, pp. 53–62). Mexico: GCAGS Transactions. http://archives.datapages.com/data/gcags/data/044/044001/0053.htm

Castagna, J. P., & Sun, S. (2006). *Comparison of spectral decomposition methods: First Break, 24,* 75–79.

Castagna, J. P., Sun, S., & Siegfried, R. W. (2003). Instantaneous spectral analysis: Detection of low-frequency shadows associated with hydrocarbons. *The Leading Edge, 22,* 120–127.

González, N., Ángeles, F., Reyes, J., Balasejus, D., Suter, A., Helfenbein, Y., Meneses, J., Puerto, C., & Audemard, F. (2004). *Choch Mulix a prolific Area on the Western Margin of the Akal Horst, Southern Gulf of Mexico: AAPG International Conference, Resumen extendido, Cancun, Mexico*. http://archives.datapages.com/data/specpubs/memoir90/CHAPTER22/CHAPTER22.HTM

Guo, H., Marfurt, K., & Liu, J. (2009). Principal component spectral analysis. *Geophysics, 74*(4), P35–P43.

Liu, J., & Marfurt, K. J. (2007). Instantaneous spectral attributes to detect channels. *Geophysics, 72*(2), P23–P31.

Marfurt, K. J., & Kirlin, R. L. (2001). Narrow-band spectral analysis and thin-bed tuning. *Geophysics, 66*(4), 1274–1283.

Martínez-Kemp, H., González-Posadas, J.F., & Bartok, P. (2005a). *Salt involvement in the Jujo-Tecominoacán Thrust Belt, Chiapas-Tabasco Región, South East Basin* (Vol. 55, pp. 520–530). Mexico: GCAGS Transactions. http://archives.datapages.com/data/gcags/data/055/055001/520_gcags550520.htm

Naseer, T. M., Shazia A., Mirza N., Farrukh H., & Shahid N. Q. (2014). Application of seismic attributes for delineation of channel geometries and analysis of various aspects in terms of lithological and structural perspectives of Lower Goru Formation, Pakistan. *International Journal of Geosciences, 5*(12), 1490–1502.

Oviedo-Pérez, A. (1998). *New exploration concept in the Salina Basin*. Southeast Mexico: AAPG Annual Convention, Abstract.

Partyka, G., Gridley, J., & Lopez, J. (1999). Interpretational applications of spectral decomposition in reservoir characterization. *The Leading Edge, 18,* 353–360.

Robles-Nolasco, J., Pliego-Vidal, E., Toledo-Bante, C., Pimienta-Lugo, M., Ortega-González, V., Martínez-Peña, B., & Heredia-Cervantes, E. (2004). *Offshore Neogene Plays, Salina del Istmo Basin*. Southeast of Mexico: Resumen extendido, AAPG International Conference, Cancún, México. http://www.searchanddiscovery.com/pdfz/documents/abstracts/2004intl_cancun/extended/A89597.pdf.html

Sinha, S., Partha, S. R., Phil, D. A., & Castagna, J. P. (2005). Spectral decomposition of seismic data with continuous-wavelet transform. *Geophysics, 70*(6), P19–P25.

Soto-Cuervo, A., Ortega-González, V., & Mora-Oropeza, G. (2004). *Present and future of the Salina del Istmo Basin and its offshore extension into the Golf of Mexico: AAPG International Conference, Resumen Extendido, Cancún, México*. http://www.searchanddiscovery.com/documents/abstracts/2004intl_cancun/extended/a91518.pdf

Stockwell, R. G., Mansinha, L., & Lowe, R. P. (1996). Localization of the complex spectrum: The S-Transform. *IEEE Transactions on Signal Processing, 44,* 998–1001.

(Received July 3, 2017, revised September 16, 2018, accepted September 18, 2018)